JOURNAL OF MATERIALS PROCESSING TECHNOLOGY 203 (2008) 389–395

journal homepage: www.elsevier.com/locate/jmatprotec

Influence of a modulated electromagnetic field on fouling in a double-pipe heat exchanger

Abdullah Shahryari, Mahmood Pakshir*

Department of Materials Science and Engineering, Shiraz University, Shiraz, Iran

ARTICLE INFO

Article history:
Received 24 November 2006
Received in revised form
12 October 2007
Accepted 22 October 2007

Keywords:
Water treatment
Fouling
Electromagnetic field
Heat transfer

ABSTRACT

In this study, the effect of a modulated electromagnetic field (MEF) on fouling in a double-pipe heat exchanger (DPHE) has been investigated. A double-loop-configuration consisting of cooling and heating water cycles was used for the experiments. The quality of heat transfer in the DPHE was studied via in situ monitoring of the fouling resistance. Moreover, the influence of cooling water linear velocity, on the MEF treatment efficiency has also been investigated. In this regard, the water flow velocities of 0.5, 0.8 and 1.3 ms^{-1} were selected. Results show that the application of the MEF on the cooling water flowing at 0.5 ms^{-1} velocity, decreased the fouling resistance in the heat exchanger by 76.3% compared to the blank (untreated) test. However, increasing the water velocity resulted in a decrease in the MEF efficiency, where 64.3% and 57.8% drop in fouling resistance of the DPHE was recorded for 0.8 and 1.3 ms^{-1} water velocities, respectively. On the other hand, the water ionic calcium (Ca^{2+}) measurements showed a significant decrease in the cooling water calcium as a result of the MEF treatment. Finally, the MEF design parameters along with the responsible mechanism for the observed results have been discussed.

1. Introduction

Fouling is defined as the accumulation of dirt, scale, corrosion products or other materials on the surfaces of the heat exchangers (Melo et al., 1987; Saunders, 1988). Presence of the dirt is associated with a further resistance to heat transfer in addition to those present due to the inherent design of the heat exchanger. The other problem, which arises from fouling is due to the reduction of the flow area while deposits have formed. These problems can cause severe localized attacks such as under-deposit corrosion and ultimately increase the maintenance and energy consumption costs in the system (Melo et al., 1987). The most common methods of water treatment for scale prevention are chemical treatment methods including application of ion exchangers or demineralizers (Cowan and Weintritt, 1976). Chemical compounds, in very small concentrations are claimed to retard calcium carbonate scale formation (Baker and Judd, 1996; Xyla and Koutsoukos, 1987). Traditional chemical methods of scale control or water softening such as pre-precipitation of scale formers with either lime or soda ash are also still used in the industries which use water as a common raw material in their processes. These chemical methods, though effective in scale control, substantially change the solution chemistry and can be prohibitively expensive (Baker and Judd, 1996). Considerable effort has also been concerned with the development of devices for electric treatment of water (Lee and Cho, 2002a; Kim and Cho, 2001), magnetic water treatment (Coey and Cass, 2001), UV radiation, as well as devices for applying ultrasonic fields on water (Dalas, 2001).

* *Corresponding author*. Present address: Department of Chemical Engineering, McGill University, 3610 University Street, Montreal, QC H3A 2B2, Canada. Tel.: +1 514 562 5055; fax: +1 514 398 6678.
E-mail address: abdullah.shahryari@mcgill.ca (A. Shahryari).
0924-0136/$ – see front matter © 2007 Elsevier B.V. All rights reserved.
doi:10.1016/j.jmatprotec.2007.10.048

Anti-scale magnetic treatment has a long and controversial history (Duffy, 1977; Donaldson and Grimes, 1988). Its major effects have been commonly assumed to be: reducing scale formation, removing existing scale or/and producing a softer and less tenacious scale (Baker and Judd, 1996; Szkatula et al., 2002; Gabrielli et al., 2001; Kobe et al., 2001). However, the reported water treatment methods are sometimes questionable due to lack of consistency and reproducibility (Szkatula et al., 2002; Busch and Busch, 1997). This is probably a consequence of variations in water composition, differences in the course of the treatment and the complexity of the processes, which occur, in the aqueous solutions (Coey and Cass, 2001; Szkatula et al., 2002). It is generally approved in literature that application of a magnetic field favors the pre-formation of calcium carbonate particles in the bulk of the scaling water, hence preventing the formation/adherence of the precipitates onto the walls of the distribution pipes and susceptible areas. These particles can be eliminated and removed by filtering the treated water (Szkatula et al., 2002; Gabrielli et al., 2001; Al-Qahtani, 1996). Y.I. Cho et al. (Lee and Cho, 2002a; Kim and Cho, 2001; Lee and Cho, 2002b) reported works on treatment of a cooling system water using electromagnets supplied by an alternative pulsating current aimed at increasing the heat transfer in a heat exchanger under closely controlled laboratory conditions. A square wave pulsing current at constant frequency of 500 Hz, creating a time varying magnetic filed inside the pipe has been employed. On the other hand, the positive contribution of magnetic field on the precipitation of calcium carbonate has attracted much attention regarding the feasibility of application of magnetic fields in order to accelerate recovering bone destructions (Azuma et al., 2000).

In the present study, we are presenting our results on the application of a modulated electromagnetic field on the circulating water to prevent fouling in a double pipe heat exchanger. The frequency and amplitude modulation (FM and AM, respectively) were applied in the triangular-wave-form current source. It will be shown that significant improvement in the heat transfer quality of the heat exchanger is achieved by introducing the proposed water treatment device. The improvement in the performance of the heat exchanger in the system will be correlated to the physicochemical phenomena induced by the applied electromagnetic field.

2. Experimental details

2.1. *Experimental setup*

The chemical composition of the cooling water is given in Table 1. The electromagnetic field was applied on the cooling water flowing through a 1.6 cm × 10 cm (D × L) copper pipe wrapped with the MEF generating coil. When the MEF was applied on the cooling water, the experiment is referred to as 'treated', whereas when the MEF is switched off during the test run, the experiment is so called 'untreated' in the text. Experiments were carried out for the treated and untreated cases at three different velocities. Different flow rates were applied to the cooling water in order to obtain linear water velocities of 0.5, 0.8 and 1.3 ms^{-1} through the pipe in which the MEF was generated. This was done through settings of the adjustable cooling water pump power. The temperature of the cooling water outlet from the heat exchanger varied depending on the water flow rate. The higher the cooling water velocity, the shorter the residence time of the water in the heat exchanger and subsequently the lower the outlet water temperature.

Table 1 – Chemical composition of the make up water

Property	Quantity
pH	7.15
Ca hardness ($mg L^{-1}$)	318
Conductivity ($\mu S cm^{-1}$)	1060
Total hardness ($mg L^{-1}$)	540
Total dissolved solids ($mg L^{-1}$)	690
LSI	0.35

All the experiments were performed using a double-loop water-recirculating setup as schematically shown in Fig. 1. It consisted of cooling and heating cycles which were composed of the following basic constituents: cooling chamber with a side-installed fan to decrease the temperature of the circulating cooling water, water heater equipped with a thermostat to keep the heating water at a constant temperature, a home-made double-pipe heat exchanger, cooling and hot water pumps, floating ball valve for automatic water feeding into the cooling cycle, flow meters and finally the thermometers at the inlet and outlet of the double pipe heat exchanger (DPHE). To avoid any deposit on the heating side of the heat transfer surface, distilled water was used as the heating water. All the piping and the water heater reservoir were insulated to minimize the heat loss. The DPHE was constituted from two concentric pipes with different dimensions as shown schematically in Fig. 2. The outer tube was made of galvanized steel where the inner tube was made of copper. The cooling water flows in the gap between the inner and the outer tubes while the heating water passes through the inner tube. In order to reduce the turbulence of water in

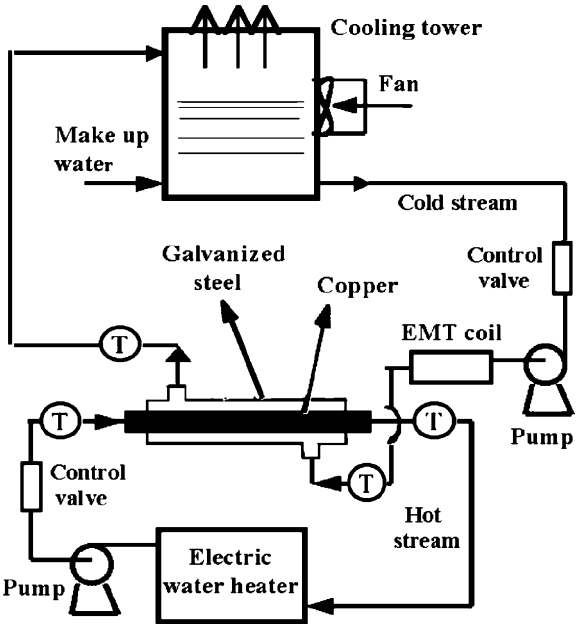

Fig. 1 – Schematic diagram of the experimental setup including the circulating water cycles.

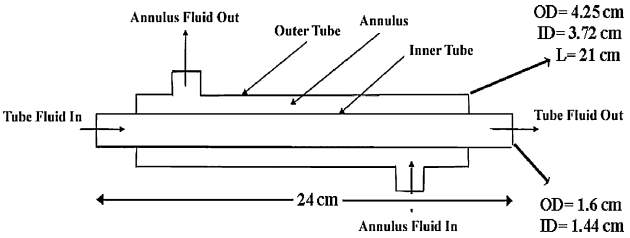

Fig. 2 – Dimensions of the double-pipe heat exchanger. The heating distilled water passes through the inner copper tube and the cooling water flows through the gap between the inner and outer tubes. The heating and cooling water flow directions are opposite.

the heat exchanger, favoring the scale formation, no baffles were embedded inside the DPHE. The make up water was fed into the system automatically using the floating valve in the cooling tower reservoir. The water was fed into the system to compensate its loss due to evaporation during air-cooling.

For each water velocity, the MEF-treated experiment was followed by the blank test (untreated). During each experiment, the cooling water Ca^{2+} content was recorded. The chemical measurements were carried out according to AWWA standard procedures. Once the experiment was finished, the deposited scales on the outer surface of the copper tube was wiped off and studied by scanning electron microscopy (SEM) using a Philips XL30 FEG (field emission gun) SEM.

2.2. *Calcium hardness measurement*

The process used in measurement of the calcium content of the water is known as "EDTA Titrimetric Method". Ethylenediamine tetraacetic acid (EDTA) and its sodium salts form a soluble complex when added to a solution of metal cations. If a small amount of a dye such as Eriochrome Black T is added to an aqueous solution containing Ca^{2+} and Mg^{2+} ions at a pH of 10 ± 0.1, the solution will become wine red. At this time if EDTA is added as a titrant, they will form complexes and at the end of this process the solution will turn from wine red to blue. This procedure is usually used to measure the total hardness of water. Through a similar trend and on a similar basis, the calcium hardness is determined. Considering that when EDTA is added to water, it combines first with calcium, the calcium hardness measurement necessitates the removal of magnesium at the first step from the water. Therefore, the pH must be raised up to high values (ca. 12–13) using NaOH solution so that all magnesium ions precipitate as hydroxide. Then, calcium hardness can be accurately measured using an indicator, which combines only with calcium. The related required reagents are sodium hydroxide (NaOH, 1N), Murexide (ammonium purpurate, as an indicator) and the standard EDTA titrant (0.01 M). Calcium hardness is then measured using the following equation:

$$\text{Calcium hardness (as mg/l } CaCO_3) = \frac{AB \times 1000}{\text{sample (ml)}} \quad (4\text{–}25)$$

where, A = mL titrant for sample, B = mg $CaCO_3$ equivalent to 1 mL EDTA at the calcium indicator end point (Rand et al., 1975).

3. Results and discussions

At the end of each 50-h-period experiment, the DPHE inner copper tube (test sample) was taken out of the heat exchanger. Fig. 3 shows the appearance of the outer surface of the heat exchanger copper tube for both treated and untreated experiments at different water velocities. An obvious difference between the appearances of the scale cumulated on the heat-exchange surfaces is observed. In the case of untreated samples, a thick deposit layer at 0.5 ms^{-1} velocity is seen on the surface. Increasing the water velocity decreases the scale deposited on the surface where the

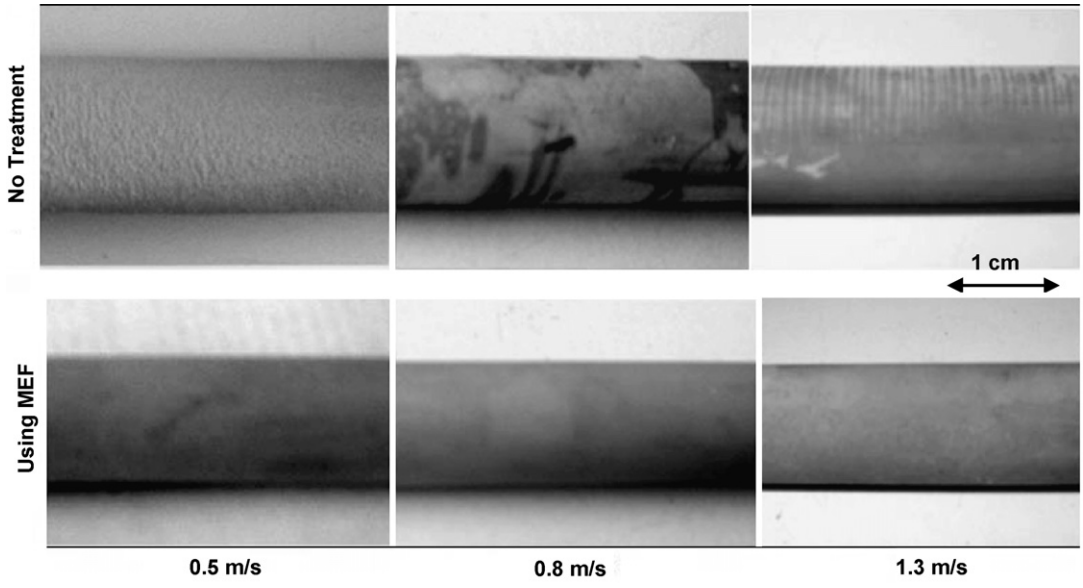

Fig. 3 – Appearance of the heat transfer surfaces at various conditions at the end of the experiments.

least scale deposition is associated with the water velocity of 1.3 ms^{-1}.

However, when the MEF is applied on the cooling water no visible heavy scale is observed on the surface but rather a very thin and easily removable form of fouling forms on the surface. Increasing the water velocity to 0.8 ms^{-1} does not result in a significant change in the appearance of the scale formed on the surface. When the velocity is increased to 1.3 ms^{-1} the synergistic influences of the MEF and water kinetic energy, results in a very clean and scale-free surface.

3.1. *Design of the electromagnetic field source*

According to Faraday's law, a variable electric field inside a coil generates a time-varying magnetic field and vice versa. The relationship between these magnetic and electric fields is generally expressed by the following equation:

$$\int E\,ds = -\frac{\partial}{\partial t}\int B\,dA \tag{1}$$

where E is the induced electric field vector, s is a line vector along the circumferential direction, B is the magnetic filed strength vector and A is the cross-sectional area of the coil (Bekefi and Barrett, 1977).

The ac triangular current-wave source was generated by means of an electronic circuit with the capability of adjustment of the current frequency. According to Eq. (1), when this ac current is applied to a coil twisted around a tube, it generates a time varying electric and magnetic field inside the coil. In order to have a modulated electromagnetic field (MEF) inside the coil, both amplitude modulation (AM) and frequency modulation (FM) were implemented in the current source. Any change in the frequency and amplitude of the current source is therefore associated with a simultaneous change in the resultant magnetic and electric fields. The source current frequency was designed to vary between 1 and 5 kHz. On the other hand the AM modulation induced a variation in the amplitude of the current between zero and a maximum value. The frequency of variation of the base current-wave amplitude was set at 20 Hz.

When a solenoid coil is supplied by an alternative (ac) current, according to the Stoke's theorem, the following relation will be established inside the coil:

$$\nabla \times \vec{E} = \frac{-\partial \vec{B}}{\partial t} \tag{2}$$

and that gives rise to the following expression (Plonsey and Collin, 1961; Rotherwell and Cloud, 2001):

$$\nabla \times \vec{E} = i\omega \vec{B} \tag{3}$$

integrating both sides of the Eq. (3) gives:

$$\int \nabla \times \vec{E} \cdot n\,ds = i\omega \int \vec{B}\, n \cdot dr \tag{4}$$

and therefore,

$$\oint_c \vec{E} \cdot d\vec{l} = i\omega Bs \tag{5}$$

solving Eq. (5) gives a simple expression relating the electric and magnetic field intensities to the applied current (Van Bladel, 1985):

$$E2\pi r = i\omega B\pi r^2 \tag{6}$$

therefore,

$$E = i\omega B\frac{r}{2} \tag{7}$$

where E is the induced electric field vector, B is the magnetic field strength vector, ω is the angular velocity of the current wave, s is the line vector along the circumferential direction, i is the imaginary value $\sqrt{-1}$ and r is the distance of the position from the centerline of the solenoid.

Removing the imaginary part from the Eq. (7) and substituting B by the term $I\mu_0 n$ gives the following useful equation (Bekefi and Barrett, 1977):

$$E = \omega I\mu_0 n\frac{r}{2} \tag{8}$$

where I is the electric current (A).

According to Eq. (8) the electric field vectors are visualized as concentric circles, the radius of which is r (distance from centerline of the solenoid). Therefore the electric field vectors distribution inside the coil, at a constant current, is only a function of the geometry of the solenoid. Fig. 4 shows the distribution of the magnetic and electric field vectors in a coil supplied by a time-varying ac current. According to Eq. (8), it is quite obvious, that changing the frequency and current amplitude would change the ω and I, respectively, which in turn, changes both electric and magnetic field intensities at any point inside the coil. However, it should be noted that the B and E vectors are always zero at the centerline and reach the maximum value at the inner wall of the coil.

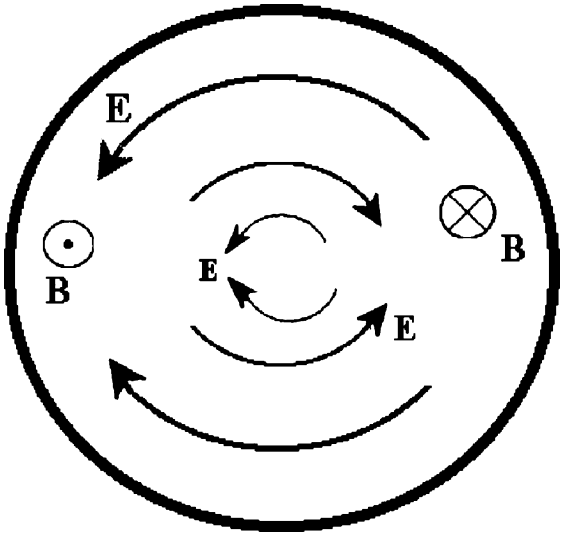

Fig. 4 – A cross-sectional profile of the generated electric and magnetic field intensity vectors supplied by an ac source in a solenoid.

3.2. *Fouling resistance*

The fouling resistance, representing the quality of heat transfer, is often expressed by the following equation:

$$R_f = \frac{1}{U_f} - \frac{1}{U_i} \quad (9)$$

where U_f is the overall heat transfer coefficient at a time after starting the test and U_i is the overall heat transfer coefficient for a clean heat exchanger. The temperature of the cooling water at the inlet of the heat exchanger was 30 °C. The cooling and heating water temperatures were monitored at four different points. Both overall heat transfer coefficients can be calculated according to this equation:

$$U = \frac{Q^o}{A\Delta T_{lm}} \quad (10)$$

While ΔT_{lm} is log-mean temperature difference and can be described using this equation:

$$\Delta T_{lm} = \frac{(T_{h,i} - T_{c,o}) - (T_{h,o} - T_{c,i})}{\ln[(T_{h,i} - T_{c,o})/(T_{h,o} - T_{c,i})]} \quad (11)$$

where $T_{c,i}$ and $T_{c,o}$ are the temperatures of the cooling water inlet and outlet and $T_{h,i}$ and $T_{h,o}$ are the temperatures of heating water inlet and outlet, respectively.

The heat transfer rate Q° can be measured from both heating and cooling circulating loops using the following equation:

$$Q^o = \left[m^o c_p (T_i - T_o)\right]_h = \left[m^o c_p (T_o - T_i)\right]_c \quad (12)$$

In the present study, the heat flux in heat exchanger was ca. 145 kWm^{-2}.

Variation of the fouling resistance with time for the treated and untreated cooling water at three different water velocities were recorded. Fig. 5 shows the dependence of the fouling resistance on time for the MEF treated and untreated cases at the water velocity of 0.5 ms^{-1}. It is clearly seen that the fouling resistance on the untreated surface increases dramatically over the first few minutes of the circulation in the system. It continuously increases with time showing a linear trend up to the end of the experiment, where it becomes ca. 4 times larger than that recorded after 1 h from the onset of the experiment. However, when the MEF is applied on the cooling water, the variation of fouling resistance demonstrates a different trend. It is seen that the resistance does not increase significantly over time and the variation demonstrates a plateau. In average, a tremendous drop of 76.3% in fouling resistance is observed when the MEF is introduced into the system. It should be noted that the efficiency of the MEF over the test period is even more pronounced at the end of the test experiment where the decrease in the fouling resistance is more than 84%.

Fig. 6 shows the result of similar investigations but for water velocities of 0.8 and 1.3 ms^{-1}. The fouling resistance for the untreated water similarly increases with time depicting a linear trend. However, the fouling resistance values at the end of the experiment are not quite identical, being less for the higher velocity. It is quite understandable taking into account that the higher water velocity is associated with a higher kinetic energy and at the same time a shorter water residence time on the heat-exchange surface. Nevertheless, the dependence of the fouling resistance on time for the treated cooling water is also different for 0.8 and 1.3 ms^{-1} water velocities. The fouling resistance values at the end of the test periods for the treated cooling water are higher than that reported at 0.5 ms^{-1}

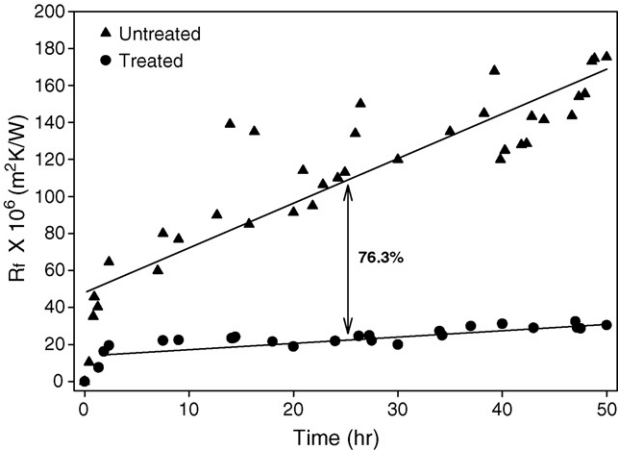

Fig. 5 – Fouling resistance variation in various conditions at 0.5 ms^{-1} flow velocity.

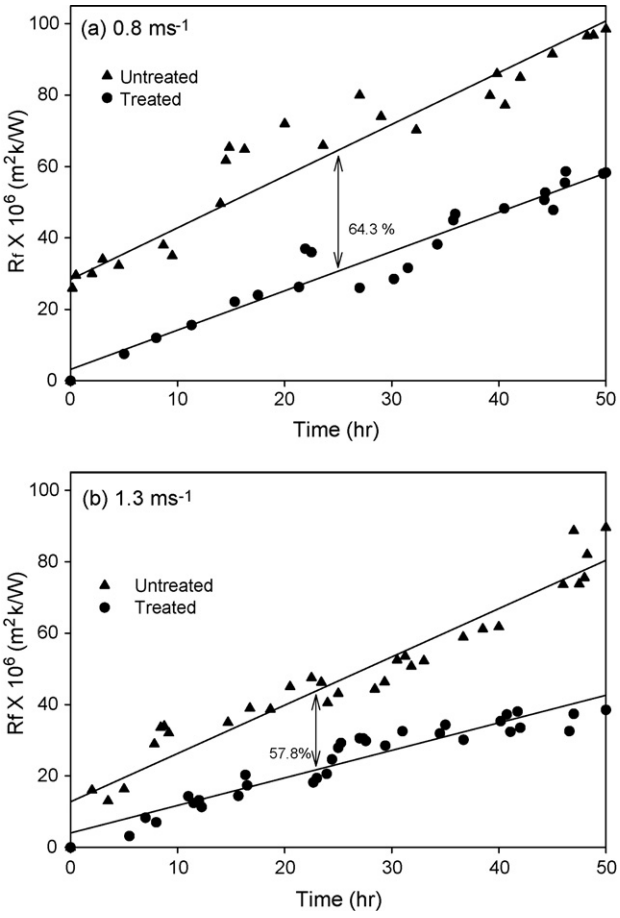

Fig. 6 – Dependence of fouling resistance on time for the treated and untreated cooling water at (a) 0.8 ms^{-1} and (b) 1.3 ms^{-1} velocities.

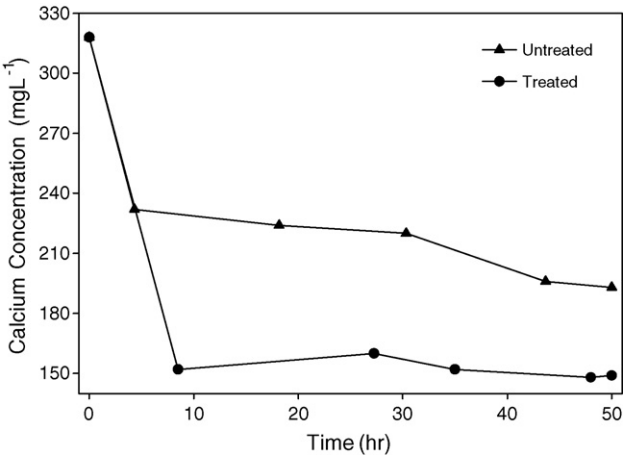

Fig. 7 – Variation of ionic calcium concentration with time for the treated and untreated cases at 0.5 ms^{-1} velocity.

velocity. This indicates that the efficiency of the MEF is dependent on the water velocity and/or the residence time in the treatment chamber. Nonetheless, applying the MEF to the system decreased the average fouling resistance of the experiments by 64.3% and 57.8% for 0.8 and 1.3 ms^{-1} water velocities, respectively.

3.3. *Water calcium content*

In order to have a better understanding of the physicochemical processes, which occur in water during the MEF treatment, the ionic content of Ca^{2+} were frequently recorded. Figs. 7 and 8 show the comparative dependence of the ionic calcium content on time for the treated and untreated cooling water. Fig. 7 shows the variation of the Ca^{2+} for the water velocity of 0.5 ms^{-1}. The $Ca^{2+}$of the untreated cooling water decreases from 318 to 232 mg L^{-1}which is equivalent to a 27% drop after the first 4 h of the experiment. It is observed that rate of the decrease in Ca^{2+} declines where at the end of the experiment, a 39% drop in the total content of Ca^{2+} is recorded.

However, when the cooling water is treated using the MEF, a more significant decrease in the Ca^{2+} in the water is noticed where a 52% drop is recorded over the first 8 h of the experiment. Measurement of the Ca^{2+} at the end of the run period shows an overall drop of 54% in the ionic calcium content of the water. Moreover, the decrease of the Ca^{2+} for the treated case was lower by 23% than that in the untreated water. Fig. 8 shows a similar behavior but for the water velocities of 0.8 and 1.3 ms^{-1}. When the cooling water velocity was 0.8 ms^{-1}, 11.5% drop was observed while, at the cooling water velocity of 1.3 ms^{-1}, the decrease in the Ca^{2+} was only 7%.

It was explained in details earlier that the electric field intensity vector at any spatial point inside the coil is a function of the geometry of the point at a fixed frequency and current. As the polarity of the source current changes (assuming that frequency and current remain constant), the vectors at that specific point in the coil take the opposite direction. On the basis of the ions charge neutrality and as a result of Columbic forces in the solution (here, cooling water) the ions are positioned in water such that the counter-charged ions are placed next to one another. Assume that at time t, the source current frequency is f where $1/2f$ is the duration for which the polarity of the current remains unchanged. When a charged particle q is exposed to an electric field E, a force will be created which according to Eq. (13) imparts the acceleration a to the particle.

$$a = \frac{qE}{m} \tag{13}$$

where m is the ion mass and q is the ion charge.

Now, for a period of time Δt, where $\Delta t < 1/2f$, the electromagnetic forces on the two counter-charged ions next to each other would cause a collision. In the next half cycle, where the polarity changes the same collision would happen alternatively between another pair of ions in the water. This enhances the possibility of an effective collision between the ions such that the bulk-precipitation of scales mainly calcium carbonate occurs. The considerable decrease in the Ca^{2+} content as a result of MEF treatment (Figs. 7 and 8) indicates that these processes occur in the cooling water while applying the MEF.

Fig. 9 shows the SEM images of the $CaCO_3$ scale-deposits formed on the heat-exchange surface from treated and

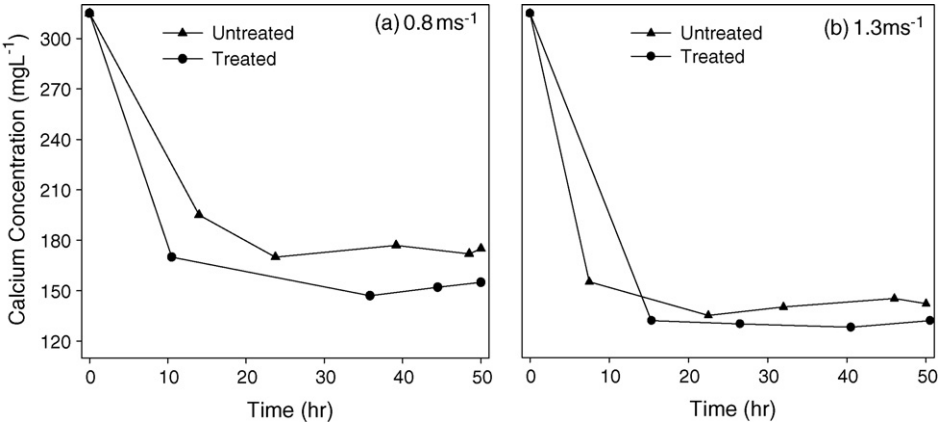

Fig. 8 – Dependence of ionic calcium concentration on time for the treated and untreated cooling water at (a) 0.8 ms^{-1} and (b) 1.3 ms^{-1} velocities.

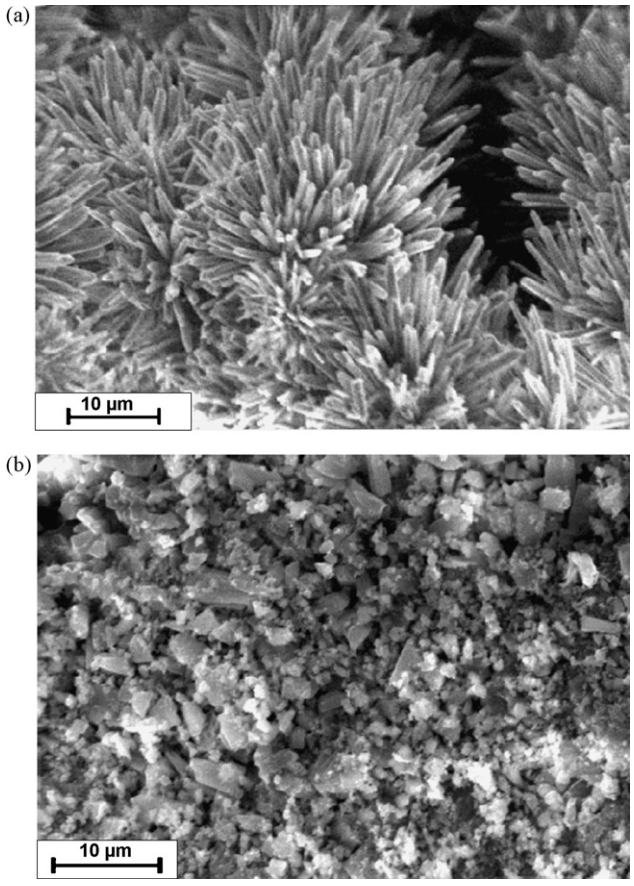

Fig. 9 – SEM image of the scale deposited on the surface of the inner tube of the double pipe heat exchanger at the end of the experiment from (a) untreated and (b) MEF treated cooling water.

untreated cooling water. When the water is not treated with the MEF, the $CaCO_3$ deposits show its common (calcite) structure which is resulted from an equilibrium state of formation of the scale. However, when the cooling water was treated by the MEF, the $CaCO_3$ deposits formed on the heat-exchange surface do not resemble those deposited out from the untreated water. The non-equilibrium condition of the $CaCO_3$ formation is concluded from the shape of the crystals formed at the surface when the water is treated with the MEF.

As discussed earlier in the text, the design parameters of the MEF-producing system are directly related to the properties and chemical composition of the cooling water. It was mentioned that when an ion with charge q is exposed to the electric field with the intensity E with m being the ion mass, a will be the acceleration that the ion would reach. This is the acceleration, which can be used along with the *motion laws* to establish a condition where the ions have maximum probability of effective collisions in the solution.

4. Conclusion

The investigation of the influence of a modulated electromagnetic field on scale deposition was carried out in a double-pipe heat-exchanger. It was found that the application of the proposed modulated electromagnetic field (MEF) could significantly decrease the fouling resistance in the heat exchanger studied at three different water velocities. Our results of the variation of the water Ca^{2+} content shows that the Ca^{2+} decreases by 23%, 11.5% and 7% at 0.5, 0.8 and 1.3 ms^{-1} water velocities, respectively. The governing mechanism of the observed effects is assumed to be enhanced collision and subsequently the higher reactivity of the ions in the water. Consequently, this could initiate the formation of the $CaCO_3$ particles in the cooling water rather than on the heat-exchange surfaces.

Acknowledgement

The financial support provided by Shiraz University is gratefully acknowledged.

REFERENCES

Al-Qahtani, H., 1996. Desalin 107, 75–81.
Azuma, N., Tajima, K., Ishizu, K., Yokoi, I., Mori, A., 2000. Pathophysiology 7, 83–89.
Baker, J.S., Judd, S.J., 1996. Water Res. 30, 247–260.
Bekefi, G., Barrett, A.H., 1977. Electromagnetic Vibration, Waves and Radiation. The MIT Press.
Busch, K.W., Busch, M.A., 1997. Desalin 109, 131–148.
Coey, J.M.D., Cass, S., 2001. J. Magn. Magn. Mater. 209, 71–74.
Cowan, J.C., Weintritt, D.J., 1976. Water Formed Scale Deposits. Culf, Houston.
Dalas, E., 2001. J. Cryst. Growth 222, 287–292.
Donaldson, J.D., Grimes, S., 1988. New Sci. 117, 43–46.
Duffy, E.A., 1977. Investigation of water treatment devices. Ph.D. Thesis. Clemson University, Clemson, SC.
Gabrielli, C., Jaouhari, R., Maurin, G., keddam, M., 2001. Water Res. 35, 3249–3259.
Kim, W.T., Cho, Y.I., 2001. Int. Commun. Heat Mass Transfer 28, 671–680.
Kobe, S., Drazic, G., Mcguiness, P.J., Strazisar, J., 2001. J. Magn. Magn. Mater. 236, 71–76.
Lee, S.H., Cho, Y.I., 2002a. Int. J. Heat Mass Transfer 45, 4163–4174.
Lee, S.H., Cho, Y.I., 2002b. Int. Commun. Heat Mass Transfer 29, 145–156.
Melo, L.F., Bott, T.R., Bernardo, C.A., 1987. Fouling science and technology E: Applied Science, NATO ASI series, vol. 145.
Plonsey, R., Collin, R.E., 1961. Principles and Application of Electromagnetic Fields. McGraw-Hill.
Rand, M.C., Greenberg, Arnold E., Taras, Michael J., 1975. Standard Methods for the Examination of Water and Wastewater, 14th ed. APHA-AWWA-WPCF.
Rotherwell, E.J., Cloud, M.J., 2001. Electromagnetics. CRC Press.
Saunders, E.A.D., 1988. Heat Exchangers. John Wiley & Sons, Inc.
Szkatula, A., Balanda, M., Kopec, M., 2002. Eur. Phys. J. Appl. Phys. 18, 41–49.
Van Bladel, J., 1985. Electromagnetic Fields. Hemisphere Publishing Corp.
Xyla, A.G., Koutsoukos, P.G., 1987. J. Chem. Soc., Faraday Trans. 183, 1477.